arXiv:1507.04008v1 [math.AP] 14 Jul 2015

NEUMANN-NEUMANN WAVEFORM RELAXATION ALGORITHM IN MULTIPLE SUBDOMAINS FOR HYPERBOLIC PROBLEMS IN 1D AND 2D

BANKIM C. MANDAL *

Abstract. We present a Waveform Relaxation (WR) version of the Neumann-Neumann algorithm for the wave equation in space-time. The method is based on a non-overlapping spatial domain decomposition, and the iteration involves subdomain solves in space-time with corresponding interface condition, followed by a correction step. Using a Fourier-Laplace transform argument, for a particular relaxation parameter, we prove convergence of the algorithm in a finite number of steps for finite time intervals. The number of steps depends on the size of the subdomains and the time window length on which the algorithm is employed. We illustrate the performance of the algorithm with numerical results, followed by a comparison with classical and optimized Schwarz WR methods.

Key words. Neumann-Neumann, Waveform Relaxation, Wave equation, Domain Decomposition.

1. Introduction. We formulate a new variant of Waveform Relaxation (WR) methods based on the Neumann-Neumann algorithm to solve hyperbolic problems in parallel computer, and present convergence results for the method. The Neumann-Neumann algorithm was introduced for solving elliptic problems by Bourgat et al. [1], see also [26] and [28]. The iteration involves solving the subdomain problems using Dirichlet interface conditions in the first step, followed by a correction step involving Neumann interface conditions. The convergence behavior of the algorithm is now well understood for elliptic problems, see for example the book [29].

To solve time-dependent problems in parallel, the following three possible classes of domain decomposition techniques exist:

- this approach consists of discretizing the problem uniformly in time with an implicit scheme to obtain a sequence of elliptic problems, which are then solved by DD methods. For this kind of technique, we refer to [2, 3]. One disadvantage of this approach is that, uniform time step across the whole domain need to be enforced, which is very restrictive for problems with variable coefficients or multiple time scales. Also this method is expensive for parallel computation, since one needs to exchange information at each time step of the discretization.
- in this approach the equation is first discretized in space, which is called the method of lines, and then one applies a waveform relaxation algorithm to solve the large system of ordinary differential equations (ODEs) obtained from the space-discretization process. Multigrid dynamic iteration [21, 16] and multisplitting algorithms [17] are some particular examples of this approach.
- in contrast to the two classical techniques above, there exist space-time domain decomposition methods, formulated at the continuous level. Here, instead of discretizing in time or in space, one decomposes the original spatial domain into smaller subdomains and considers each subproblem as posed in both space and time; then the subproblems are solved iteratively communicating information at the interfaces between subdomains. This permits the use of different numerical methods in different subdomains. At each iteration, one solves the space-time subproblem over the entire time interval of

---

[*] Department of Mathematical Sciences, Michigan Technological University, USA (`bmandal@mtu.edu`).

interest, before communicating interface data across subdomains. Thus one saves communication time while computing in parallel computer. For this approach, see [14, 15, 4, 6, 24] for parabolic problems, and [8, 5, 7] for hyperbolic problems.

In this article, we focus on the WR-type algorithm as it allows different discretizations in different space-time subdomains. WR methods have their origin in the work of Picard [25] and Lindelöf [20] in the late 19th century. Lelarasmee, Ruehli and Sangiovanni-Vincentelli [19] rediscovered WR as a parallel method for the solution of ODEs.

In a different viewpoint, the WR-type methods can be seen as an extension of DD methods for elliptic PDEs. The systematic extension of the classical Schwarz method to time-dependent parabolic problems was started in [14, 15]; later optimized SWR methods have been introduced to achieve faster convergence or convergence with no overlap, see [6] for parabolic problems, and [8] for hyperbolic problems. Recently, we extended the substructuring methods, namely the Dirichlet-Neumann and Neumann-Neumann methods, to space-time problems; for parabolic problems see [13, 23, 18, 11, 22], and for hyperbolic problems see [12, 11, 22]. We analyzed for the heat equation to prove that on finite time intervals, the Dirichlet-Neumann Waveform Relaxation (DNWR) and the Neumann-Neumann Waveform Relaxation (NNWR) methods converge superlinearly for an optimal choice of the relaxation parameter. On the contrary for the wave equation, these methods with a two-subdomains decomposition converge in a finite no of steps, see [11]. In this paper, we propose the NNWR method with many subdomains decomposition for hyperbolic problems and analyze the method for the Wave equation in one and two space dimensions. We analyze the method in the continuous setting to ensure the understanding of the asymptotic behavior of the methods in the case of fine grids.

We consider the following hyperbolic PDE on a bounded domain $\Omega \subset \mathbb{R}^d, 0 < t < T$, $d = 1, 2, 3$, with a smooth boundary as our guiding example,

$$\begin{array}{rcll} \frac{\partial^2 u}{\partial t^2} - c^2(\boldsymbol{x})\Delta u & = & f(\boldsymbol{x}, t), & \boldsymbol{x} \in \Omega, 0 < t < T, \\ u(\boldsymbol{x}, 0) & = & u_0(\boldsymbol{x}), & \boldsymbol{x} \in \Omega, \\ u_t(\boldsymbol{x}, 0) & = & v_0(\boldsymbol{x}), & \boldsymbol{x} \in \Omega, \\ u(\boldsymbol{x}, t) & = & g(\boldsymbol{x}, t), & \boldsymbol{x} \in \partial\Omega, 0 < t < T, \end{array} \tag{1.1}$$

with $c(\boldsymbol{x})$ being a positive function.

We introduce in Section 2 the non-overlapping NNWR algorithm with multiple subdomains for the model problem (1.1), and then analyze its convergence for the one dimensional wave equation. In Section 3 we present convergence result of the NNWR for multiple subdomains in 2D. Our convergence analysis shows that both the NNWR algorithm converge in a finite no of steps for finite time intervals, $T < \infty$. Finally we present numerical results in Section 4, which illustrate our analysis.

2. NNWR for multiple subdomains.

In this section we define the Neumann-Neumann Waveform Relaxation (NNWR) method with many subdomains for the model problem (1.1) on the space-time domain $\Omega \times (0, T)$ with Dirichlet data given on $\partial\Omega$. This can be treated as a generalization of the NNWR algorithm for two subdomains, for which see [12]. The method starts with a non-overlapping spatial domain decomposition, and the iteration involves subdomain solves in space time with corresponding interface condition, followed by a correction step.

2.1. NNWR algorithm.

Suppose the spatial domain Ω is partitioned into N non-overlapping subdomains $\{\Omega_i,\ 1 \leq i \leq N\}$, as illustrated in the left panel of

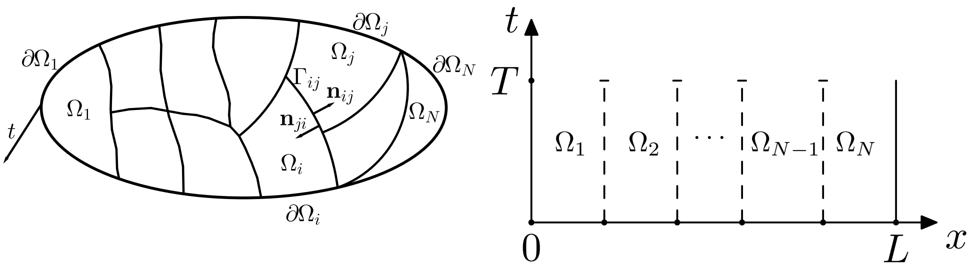

Fig. 2.1: Splitting into many non-overlapping subdomains

Figure 2.1. For $i = 1, \dots, N$ set $\Gamma_i := \partial\Omega_i \setminus \partial\Omega$, $\Lambda_i := \{j \in \{1, \dots, N\} : \Gamma_i \cap \Gamma_j$ has nonzero measure$\}$ and $\Gamma_{ij} := \partial\Omega_i \cap \partial\Omega_j$, so that the interface of Ω_i can be rewritten as $\Gamma_i = \bigcup_{j\in\Lambda_i} \Gamma_{ij}$. We denote by u_i the restriction of the solution u of (1.1) to Ω_i and by $\boldsymbol{n}_{ij}$ the unit outward normal for Ω_i on the interface Γ_{ij}. The NNWR algorithm for the model problem (1.1) starts with an initial guess $w_{ij}^0(\boldsymbol{x}, t)$ along the interfaces $\Gamma_{ij} \times (0, T)$, $j \in \Lambda_i$, $i = 1, \dots, N$, and then performs the following two-step iteration: one first solves Dirichlet subproblems on each Ω_i in parallel,

$$\begin{array}{rcll} \partial_{tt}u_i^k - c^2(\boldsymbol{x})\Delta u_i^k &=& f, & \text{in } \Omega_i, \\ u_i^k(\boldsymbol{x},0) &=& u_0(\boldsymbol{x}), & \text{in } \Omega_i, \\ \partial_t u_i^k(\boldsymbol{x},0) &=& v_0(\boldsymbol{x}), & \text{in } \Omega_i, \\ u_i^k &=& g, & \text{on } \partial\Omega_i \setminus \Gamma_i, \\ u_i^k &=& w_{ij}^{k-1}, & \text{on } \Gamma_{ij}, j \in \Lambda_i. \end{array} \tag{2.1}$$

One then solves Neumann subproblems on all subdomains,

$$\begin{array}{rcll} \partial_{tt}\varphi_i^k - c^2(\boldsymbol{x})\Delta \varphi_i^k &=& 0, & \text{in } \Omega_i, \\ \varphi_i^k(\boldsymbol{x},0) &=& 0, & \text{in } \Omega_i, \\ \partial_t \varphi_i^k(\boldsymbol{x},0) &=& 0, & \text{in } \Omega_i, \\ \varphi_i^k &=& 0, & \text{on } \partial\Omega_i \setminus \Gamma_i, \\ \partial_{\boldsymbol{n}_{ij}}\varphi_i^k &=& \partial_{\boldsymbol{n}_{ij}}u_i^k + \partial_{\boldsymbol{n}_{ji}}u_j^k, & \text{on } \Gamma_{ij}, j \in \Lambda_i. \end{array} \tag{2.2}$$

with the updating condition

$$w_{ij}^k(\boldsymbol{x},t) = w_{ij}^{k-1}(\boldsymbol{x},t) - \theta\left(\varphi_i^k\left|_{\Gamma_{ij}\times(0,T)} + \varphi_j^k\right|_{\Gamma_{ij}\times(0,T)}\right), \tag{2.3}$$

where $\theta \in (0, 1]$ is a relaxation parameter.

2.2. Convergence analysis for 1D. We prove our convergence result for the one dimensional wave equation with constant speed, $c(x) = c$ on the domain $\Omega := (0, L)$ with boundary conditions $u(0, t) = g_0(t)$ and $u(L, t) = g_L(t)$, which in turn become zeros as we consider the error equations, $f(x, t) = 0, g_0(t) = g_L(t) = 0 = u_0(x) = v_0(x)$. We decompose Ω into non-overlapping subdomains $\Omega_i := (x_{i-1}, x_i)$, $i = 1, \dots, N$, as shown in the right panel of Figure 2.1, and define the subdomain length $h_i := x_i - x_{i-1}$, and $h_{\min} := \min_{1\le i\le N} h_i$. Our initial guess is denoted by $\left\{w_i^0(t)\right\}_{i=1}^{N-1}$ on the interfaces $\{x = x_i\} \times (0, T)$, and for sake of consistency we denote

$w_0^k(t) = w_N^k(t) = 0$ for all k. We then obtain

$$\begin{array}{rcll rcll}
\partial_{tt}u_i^k - c^2\partial_{xx}u_i^k &=& 0, & \text{in } \Omega_i, & \partial_{tt}\varphi_i^k - c^2\partial_{xx}\varphi_i^k &=& 0, & \text{in } \Omega_i,\\
u_i^k(x,0) &=& 0, & \text{in } \Omega_i, & \varphi_i^k(x,0) &=& 0, & \text{in } \Omega_i,\\
\partial_t u_i^k(x,0) &=& 0, & \text{in } \Omega_i, & \partial_t\varphi_i^k(x,0) &=& 0, & \text{in } \Omega_i,\\
u_i^k(x_{i-1},t) &=& w_{i-1}^{k-1}(t), & & -\partial_x\varphi_i^k(x_{i-1},t) &=& (\partial_x u_{i-1}^k - \partial_x u_i^k)(x_{i-1},t), &\\
u_i^k(x_i,t) &=& w_i^{k-1}(t), & & \partial_x\varphi_i^k(x_i,t) &=& (\partial_x u_i^k - \partial_x u_{i+1}^k)(x_i,t), &
\end{array} \tag{2.4}$$

except for the first and last subdomains, where the Neumann conditions in the Neumann step are replaced by homogeneous Dirichlet conditions along the physical boundaries. The updated interface values for the next step will be

$$w_i^k(t) = w_i^{k-1}(t) - \theta\left(\varphi_i^k(x_i,t) + \varphi_{i+1}^k(x_i,t)\right). \tag{2.5}$$

We start by applying the Laplace transform to the homogeneous Dirichlet subproblems in (2.4), and obtain

$$s^2\hat{u}_i - c^2\hat{u}_{i,xx} = 0, \quad \hat{u}_i(x_{i-1},s) = \hat{w}_{i-1}(s), \quad \hat{u}_i(x_i,s) = \hat{w}_i(s),$$

for $i = 2, ..., N-1$. Set $\gamma_i = \cosh\left(h_i s/c\right), \sigma_i = \sinh\left(h_i s/c\right)$. These subdomain problems have the solutions

$$\hat{u}_i(x,s) = \frac{1}{\sigma_i}\left(\hat{w}_i(s)\sinh\left((x-x_{i-1})s/c\right) + \hat{w}_{i-1}(s)\sinh\left((x_i-x)s/c\right)\right).$$

Next we apply the Laplace transform to the Neumann subproblems in (2.4) for subdomains not touching the physical boundary, and obtain

$$\hat{\varphi}_i(x,s) = C_i(s)\cosh\left((x-x_{i-1})s/c\right) + D_i(s)\cosh\left((x_i-x)s/c\right),$$

where

$$\begin{aligned}
C_i &= \frac{1}{\sigma_i}\left(\hat{w}_i\left(\frac{\gamma_i}{\sigma_i} + \frac{\gamma_{i+1}}{\sigma_{i+1}}\right) - \frac{\hat{w}_{i-1}}{\sigma_i} - \frac{\hat{w}_{i+1}}{\sigma_{i+1}}\right),\\
D_i &= \frac{1}{\sigma_i}\left(\hat{w}_{i-1}\left(\frac{\gamma_i}{\sigma_i} + \frac{\gamma_{i-1}}{\sigma_{i-1}}\right) - \frac{\hat{w}_{i-2}}{\sigma_{i-1}} - \frac{\hat{w}_i}{\sigma_i}\right).
\end{aligned}$$

We therefore obtain for $i = 2, ..., N-2$, at iteration k

$$\begin{aligned}
\hat{w}_i^k(s) &= \hat{w}_i^{k-1}(s) - \theta\left(\hat{\varphi}_i^k(x_i,s) + \hat{\varphi}_{i+1}^k(x_i,s)\right)\\
&= \hat{w}_i^{k-1}(s) - \theta\left(C_i\gamma_i + D_i + C_{i+1} + D_{i+1}\gamma_{i+1}\right).
\end{aligned}$$

Using the identity $\gamma_i^2 - 1 = \sigma_i^2$ and simplifying, we get

$$\begin{aligned}
\hat{w}_i^k = \hat{w}_i^{k-1} - \theta\Bigg(&\hat{w}_i^{k-1}\left(2 + \frac{2\gamma_i\gamma_{i+1}}{\sigma_i\sigma_{i+1}}\right) + \frac{\hat{w}_{i+1}^{k-1}}{\sigma_{i+1}}\left(\frac{\gamma_{i+2}}{\sigma_{i+2}} - \frac{\gamma_i}{\sigma_i}\right)\\
&+ \frac{\hat{w}_{i-1}^{k-1}}{\sigma_i}\left(\frac{\gamma_{i-1}}{\sigma_{i-1}} - \frac{\gamma_{i+1}}{\sigma_{i+1}}\right) - \frac{\hat{w}_{i+2}^{k-1}}{\sigma_{i+1}\sigma_{i+2}} - \frac{\hat{w}_{i-2}^{k-1}}{\sigma_i\sigma_{i-1}}\Bigg).
\end{aligned} \tag{2.6}$$

For $i=1$ and $i=N$, the Neumann conditions on the physical boundary are replaced by homogeneous Dirichlet conditions $\varphi_1(0,t)=0$ and $\varphi_N(L,t)=0$, $t>0$. For these two subdomains, we obtain as solution after a Laplace transform

$$\hat{\varphi}_1(x,s)=\frac{1}{\gamma_1}\left(\hat{w}_1\left(\frac{\gamma_1}{\sigma_1}+\frac{\gamma_2}{\sigma_2}\right)-\frac{\hat{w}_2}{\sigma_2}\right)\sinh\left((x-x_0)s/c\right),$$
$$\hat{\varphi}_N(x,s)=\frac{1}{\gamma_N}\left(\hat{w}_{N-1}\left(\frac{\gamma_{N-1}}{\sigma_{N-1}}+\frac{\gamma_N}{\sigma_N}\right)-\frac{\hat{w}_{N-2}}{\sigma_{N-1}}\right)\sinh\left((x_N-x)s/c\right),$$

and thus the recurrence relations on the first interface is

$$\hat{w}_1^k=\hat{w}_1^{k-1}-\theta\left(\hat{w}_1^{k-1}\left(2+\frac{\gamma_1\gamma_2}{\sigma_1\sigma_2}+\frac{\sigma_1\gamma_2}{\gamma_1\sigma_2}\right)+\frac{\hat{w}_2^{k-1}}{\sigma_2}\left(\frac{\gamma_3}{\sigma_3}-\frac{\sigma_1}{\gamma_1}\right)-\frac{\hat{w}_3^{k-1}}{\sigma_2\sigma_3}\right), \tag{2.7}$$

and on the last interface, we obtain

$$\begin{aligned}\hat{w}_{N-1}^k=\hat{w}_{N-1}^{k-1}-\theta\Bigg(\hat{w}_{N-1}^{k-1}\left(2+\frac{\gamma_{N-1}\gamma_N}{\sigma_{N-1}\sigma_N}+\frac{\sigma_N\gamma_{N-1}}{\gamma_N\sigma_{N-1}}\right)&\\+\frac{\hat{w}_{N-2}^{k-1}}{\sigma_{N-1}}\left(\frac{\gamma_{N-2}}{\sigma_{N-2}}-\frac{\sigma_N}{\gamma_N}\right)-\frac{\hat{w}_{N-3}^{k-1}}{\sigma_{N-1}\sigma_{N-2}}\Bigg).&\end{aligned} \tag{2.8}$$

We have the following convergence result for NNWR in 1D:

Theorem 2.1 (Convergence of NNWR for multiple subdomains). *Let $\theta=1/4$. Then the NNWR algorithm (2.4)-(2.5) converges in $k+1$ iterations, if the time window length T satisfies $T/k\le 2h_{\min}/c$, c being the wave speed.*

Proof. With $\theta=1/4$ the updating condition (2.6) becomes

$$\begin{aligned}\hat{w}_i^k(s)=-\frac{1}{4}\big(\hat{t}_{i,i}\hat{w}_i^{k-1}(s)+\hat{t}_{i,i+1}\hat{w}_{i+1}^{k-1}(s)+\hat{t}_{i,i-1}\hat{w}_{i-1}^{k-1}(s)&\\-\hat{t}_{i,i+2}\hat{w}_{i+2}^{k-1}(s)-\hat{t}_{i,i-2}\hat{w}_{i-2}^{k-1}(s)\big),&\end{aligned} \tag{2.9}$$

where we defined $\hat{t}_{i,i}:=\frac{2}{\sigma_i\sigma_{i+1}}(\gamma_i\gamma_{i+1}-\sigma_i\sigma_{i+1})$, $\hat{t}_{i,i+1}:=\frac{(\sigma_i\gamma_{i+2}-\gamma_i\sigma_{i+2})}{\sigma_i\sigma_{i+1}\sigma_{i+2}}$, $\hat{t}_{i,i-1}:=\frac{(\sigma_{i+1}\gamma_{i-1}-\gamma_{i+1}\sigma_{i-1})}{\sigma_i\sigma_{i-1}\sigma_{i+1}}$, $\hat{t}_{i,i+2}:=\frac{1}{\sigma_{i+1}\sigma_{i+2}}$, and $\hat{t}_{i,i-2}:=\frac{1}{\sigma_i\sigma_{i-1}}$. Similarly, we obtain for (2.7)

$$\hat{w}_1^k(s)=-\frac{1}{4}\left(\hat{t}_{1,1}\hat{w}_1^{k-1}(s)+\hat{t}_{1,2}\hat{w}_2^{k-1}(s)-\hat{t}_{1,3}\hat{w}_3^{k-1}(s)\right), \tag{2.10}$$

where we defined $\hat{t}_{1,1}:=\left(\frac{\sigma_1\gamma_2}{\gamma_1\sigma_2}+\frac{\gamma_1\gamma_2}{\sigma_1\sigma_2}-2\right)$, $\hat{t}_{1,2}=\frac{1}{\sigma_2}\left(\frac{\gamma_3}{\sigma_3}-\frac{\sigma_1}{\gamma_1}\right)$ and $\hat{t}_{1,3}=\frac{1}{\sigma_2\sigma_3}$. From (2.8), we obtain

$$\hat{w}_{N-1}^k(s)=-\frac{1}{4}\left(\hat{t}_{N-1,N-1}\hat{w}_{N-1}^{k-1}(s)+\hat{t}_{N-1,N-2}\hat{w}_{N-2}^{k-1}(s)-\hat{t}_{N-1,N-3}\hat{w}_{N-3}^{k-1}(s)\right), \tag{2.11}$$

where we defined $\hat{t}_{N-1,N-1}=\left(\frac{\sigma_{N-1}\gamma_{N-2}}{\gamma_{N-1}\sigma_{N-2}}+\frac{\gamma_{N-1}\gamma_{N-2}}{\sigma_{N-1}\sigma_{N-2}}-2\right)$, $\hat{t}_{N-1,N-3}=\frac{1}{\sigma_{N-2}\sigma_{N-3}}$ and $\hat{t}_{N-1,N-2}=\frac{1}{\sigma_{N-2}}\left(\frac{\gamma_{N-3}}{\sigma_{N-3}}-\frac{\sigma_{N-1}}{\gamma_{N-1}}\right)$. Note that $\hat{t}_{i,i+2}=\hat{t}_{i+2,i},\hat{t}_{i,i+1}=-\hat{t}_{i+1,i}$. So by induction on (2.9)-(2.10) we can write

$$\hat{w}_i^k(s)=\sum_{j=-2n}^{2n}\left(-\tfrac{1}{4}\right)^n p_{i+j}^n\left(\hat{t}_{i+j,i+j-2},\hat{t}_{i+j,i+j-1},\ldots,\hat{t}_{i,i},\ldots,\hat{t}_{i+j,i+j+1},\hat{t}_{i+j,i+j+2}\right)\hat{w}_{i+j}^{k-n}(s), \tag{2.12}$$

and

$$\hat{w}_1^k(s) = \sum_{j=0}^{2n} \left(-\frac{1}{4}\right)^n p_{1+j}^n \left(\hat{t}_{1,1}, \ldots, \hat{t}_{1+j,2+j}, \hat{t}_{1+j,3+j}\right) \, \hat{w}_{1+j}^{k-n}(s), \tag{2.13}$$

where the coefficients p_{i+j}^n are homogeneous polynomials of degree n. A similar expression holds for $\hat{w}_{N-1}^k(s)$. Now expanding hyperbolic functions into infinite binomial series, we obtain

$$\begin{aligned}\hat{t}_{i,i} = \frac{2\cosh\left((h_i - h_{i+1})s/c\right)}{\sinh(h_i s/c)\sinh(h_{i+1}s/c)} = 4\left(e^{-2h_i s/c} + e^{-2h_{i+1}s/c}\right)\Bigg[1 + \sum_{m=1}^{\infty} e^{-2h_i ms/c} \\ + \sum_{n=1}^{\infty} e^{-2h_{i+1}ns/c} + \sum_{m=1}^{\infty}\sum_{n=1}^{\infty} e^{-2(mh_i + nh_{i+1})s/c}\Bigg],\end{aligned}$$

$$\begin{aligned}\hat{t}_{i,i+1} = \frac{\sinh\left((h_i - h_{i+2})s/c\right)}{\sinh(h_i s/c)\sinh(h_{i+1}s/c)\sinh(h_{i+2}s/c)} = 4\Bigg[1 + \sum_{l=1}^{\infty} e^{-\frac{2lsh_i}{c}} + \sum_{m=1}^{\infty} e^{-\frac{2msh_{i+1}}{c}} \\ + \sum_{n=1}^{\infty} e^{-\frac{2nsh_{i+2}}{c}} + \sum_{m=1}^{\infty}\sum_{n=1}^{\infty}\left\{e^{-\frac{2(mh_i + nh_{i+1})s}{c}} + e^{-\frac{2(mh_{i+1} + nh_{i+2})s}{c}} + e^{-\frac{2(mh_{i+1} + nh_{i+2})s}{c}}\right\} \\ + \sum_{l=1}^{\infty}\sum_{m=1}^{\infty}\sum_{n=1}^{\infty} e^{-\frac{2(lh_i + mh_{i+1} + nh_{i+2})s}{c}}\Bigg]\left(e^{-\frac{(h_{i+1} + 2h_{i+2})s}{c}} - e^{-\frac{(h_{i+1} + 2h_i)s}{c}}\right),\end{aligned}$$

$$\begin{aligned}\hat{t}_{i,i+2} = \frac{1}{\sinh(h_{i+1}s/c)\sinh(h_{i+2}s/c)} = 4e^{-(h_{i+1} + h_{i+2})s/c}\Bigg[1 + \sum_{m=1}^{\infty} e^{-2msh_{i+1}/c} \\ + \sum_{n=1}^{\infty} e^{-2nsh_{i+2}/c} + \sum_{m=1}^{\infty}\sum_{n=1}^{\infty} e^{-2(mh_{i+1} + nh_{i+2})s/c}\Bigg],\end{aligned}$$

$$\begin{aligned}\hat{t}_{1,1} = \frac{2\cosh\left((2h_1 - h_2)s/c\right)}{\sinh(2h_1 s/c)\sinh(h_2 s/c)} = 4\left(e^{-4h_1 s/c} + e^{-2h_2 s/c}\right)\Bigg[1 + \sum_{m=1}^{\infty} e^{-4msh_1/c} \\ + \sum_{n=1}^{\infty} e^{-2nsh_2/c} + \sum_{m=1}^{\infty}\sum_{n=1}^{\infty} e^{-2(2mh_1 + nh_2)s/c}\Bigg],\end{aligned}$$

$$\begin{aligned}\hat{t}_{1,2} = \frac{\cosh\left((h_1 - h_3)s/c\right)}{\cosh(h_1 s/c)\sinh(h_2 s/c)\sinh(h_3 s/c)} = 4\Bigg[1 + \sum_{l=1}^{\infty}(-1)^l e^{-\frac{2lsh_1}{c}} + \sum_{m=1}^{\infty} e^{-\frac{2msh_2}{c}} \\ + \sum_{n=1}^{\infty} e^{-\frac{2nsh_3}{c}} + \sum_{m=1}^{\infty}\sum_{n=1}^{\infty}\left\{(-1)^m e^{-\frac{2(mh_1 + nh_2)s}{c}} + (-1)^m e^{-\frac{2(mh_1 + nh_3)s}{c}} + e^{-\frac{2(mh_2 + nh_3)s}{c}}\right\} \\ + \sum_{l=1}^{\infty}\sum_{m=1}^{\infty}\sum_{n=1}^{\infty}(-1)^l e^{-2(lh_1 + mh_2 + nh_3)s/c}\Bigg]\left(e^{-(2h_1 + h_2)s/c} + e^{-(h_2 + 2h_3)s/c}\right).\end{aligned}$$

The argument also holds similarly for the terms $\hat{t}_{i,i-1}$, $\hat{t}_{i,i-2}$, $\hat{t}_{1,3}$, $\hat{t}_{N-1,N-1}$, $\hat{t}_{N-1,N-2}$, $\hat{t}_{N-1,N-3}$. Now using these expressions we can write (2.12)-(2.13) as

$$\hat{w}_i^k(s) = (-1)^k \left[\left(e^{-2ksh_i/c} + e^{-2ksh_{i+1}/c} \right) \hat{w}_i^0(s) + \sum_{j=-2k}^{2k} q_{i+j}^k(s)\, \hat{w}_{i+j}^0(s) \right], \tag{2.14}$$

and

$$\hat{w}_1^k(s) = (-1)^k \left[\left(e^{-4h_1ks/c} + e^{-2h_2ks/c} \right) \hat{w}_1^0(s) + \sum_{j=0}^{2k} r_{1+j}^k(s)\, \hat{w}_{1+j}^0(s) \right], \tag{2.15}$$

where $q_{i+j}^k(s)$ and $r_{1+j}^k(s)$ are linear combinations of terms of the form e^{-sm} with $m \geq 2kh_l/c$ for some $l \in \{1, 2, \dots N\}$. A similar expression holds for $\hat{w}_{N-1}^k(s)$. We now recall the shifting property of Laplace transform

$$\mathcal{L}^{-1}\left\{ e^{-\alpha s} \hat{f}(s) \right\} = H(t-\alpha) f(t-\alpha), \tag{2.16}$$

where $H(t) := \begin{cases} 1, & t > 0, \\ 0, & t \leq 0. \end{cases}$ is the Heaviside step function. We use (2.16) to back transform (2.14)-(2.15) and obtain

$$w_i^k(t) = (-1)^k \left[w_i^0\left(t - \frac{2kh_i}{c}\right) H\left(t - \frac{2kh_i}{c}\right) + w_i^0\left(t - \frac{2kh_{i+1}}{c}\right) H\left(t - \frac{2kh_{i+1}}{c}\right) \right.$$
$$\left. + \text{ other terms} \right],$$

$$w_1^k(t) = (-1)^k \left[w_1^0\left(t - \frac{4kh_1}{c}\right) H\left(t - \frac{4kh_1}{c}\right) + w_1^0\left(t - \frac{2kh_2}{c}\right) H\left(t - \frac{2kh_2}{c}\right) \right.$$
$$\left. + \text{ other terms} \right]$$

and a similar expression for $w_{N-1}^k(t)$. So for $T \leq 2kh_{\min}/c$, we get $w_i^k(t) = 0$ for all i, and the conclusion follows. ∎

Remark 2.2. *The shifting property of Laplace transform (2.16) is the reason behind the finite step convergence of the DNWR for a particular value of the parameter θ. The right hand side of (2.16) becomes identically zero for $t \leq \alpha$, so that for sufficiently small time window length T (e.g., $T \leq \alpha$) the error becomes zero and leads to convergence in the next iteration. In Figure 2.2 we plot $\mathcal{L}^{-1}\left\{\hat{f}(s)\right\}$ with $f(t) = \sin(t)$ on the left, and show the effect of time-shifting on the right.*

3. Analysis of NNWR algorithm in 2D.

We now formulate and analyze the NNWR algorithm for the two-dimensional wave equation

$$\partial_{tt} u - c^2 \Delta u = f(x,y,t), \quad (x,y) \in \Omega = (l, L) \times (0, \pi),\ t \in (0, T]$$

with initial condition $u(x,y,0) = u_0(x,y), \partial_t u(x,y,0) = v_0(x,y)$ and Dirichlet boundary conditions. To define the Neumann-Neumann algorithm, we decompose Ω into strips of the form $\Omega_i = (x_{i-1}, x_i) \times (0, \pi)$, $l = x_0 < x_1 < \cdots < x_N = L$. We define the subdomain width $h_i := x_i - x_{i-1}$, and $h_{\min} := \min_{1 \leq i \leq N} h_i$. Also we directly

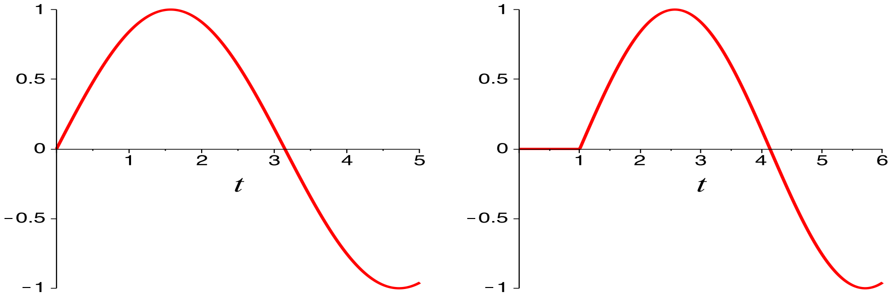

Fig. 2.2: Example of time-shifting for the function $f(t) = \sin(t)$: $\mathcal{L}^{-1}\left\{\hat{f}(s)\right\}$ on the left, and $\mathcal{L}^{-1}\left\{e^{-s}\hat{f}(s)\right\}$ on the right

consider the error equations with $f(x, y, t) = 0, u_0(x, y) = 0 = v_0(x, y)$ and homogeneous Dirichlet boundary conditions. Given initial guesses $\left\{w_i^0(y,t)\right\}_{i=1}^{N-1}$ along the interface $\{x = x_i\}$, the NNWR algorithm, as a particular case of (2.1)-(2.2)-(2.3), is given by performing iteratively for $k = 1, 2, \ldots$ and for $i = 1, \ldots, N$ the Dirichlet and Neumann steps

$$\begin{aligned} \partial_{tt}u_i^k - c^2\Delta u_i^k &= 0, \quad \text{in } \Omega_i, & \partial_{tt}\varphi_i^k - c^2\Delta\varphi_i^k &= 0, \quad \text{in } \Omega_i,\\ u_i^k(x,y,0) &= 0, & \varphi_i^k(x,y,0) &= 0,\\ \partial_t u_i^k(x,y,0) &= 0, & \partial_t\varphi_i^k(x,y,0) &= 0,\\ u_i^k(x_{i-1},y,t) &= w_{i-1}^{k-1}(y,t), & \partial_{n_i}\varphi_i^k(x_{i-1},y,t) &= (\partial_{n_{i-1}}u_{i-1}^k + \partial_{n_i}u_i^k)(x_{i-1},y,t),\\ u_i^k(x_i,y,t) &= w_i^{k-1}(y,t), & \partial_{n_i}\varphi_i^k(x_i,y,t) &= (\partial_{n_{i-1}}u_{i-1}^k + \partial_{n_i}u_i^k)(x_i,y,t),\\ u_i^k(x,0,t) &= u_i^k(x,\pi,t) = 0, & \varphi_i^k(x,0,t) &= \varphi_i^k(x,\pi,t) = 0, \end{aligned} \tag{3.1}$$

except for the first and last subdomain, where in the Neumann step the Neumann conditions are replaced by homogeneous Dirichlet conditions along the physical boundaries. The update conditions are defined as

$$w_i^k(y,t) = w_i^{k-1}(y,t) - \theta\left(\varphi_i^k(x_i,y,t) + \varphi_{i+1}^k(x_i,y,t)\right).$$

We perform a Fourier transform along the y direction to reduce the original problem into a collection of one-dimensional problems. Using a Fourier sine series along the y-direction, we get

$$u_i^k(x,y,t) = \sum_{n\geq 1} U_i^k(x,n,t)\sin(ny)$$

where

$$U_i^k(x,n,t) = \frac{2}{\pi}\int_0^\pi u_i^k(x,\eta,t)\sin(n\eta)d\eta.$$

The NNWR algorithm (3.1) therefore becomes a sequence of 1D problems for each n,

$$\frac{\partial^2 U_i^k}{\partial t^2}(x,n,t) - c^2\frac{\partial^2 U_i^k}{\partial x^2}(x,n,t) + c^2n^2U_i^k(x,n,t) = 0, \tag{3.2}$$

with the boundary conditions for $U_i^k(x,n,t)$. We now define

$$\chi(\alpha,\beta,t) := \mathcal{L}^{-1}\left\{\exp\left(-\beta\sqrt{s^2+\alpha^2}\right)\right\}, \quad \mathrm{Re}(s)>0, \tag{3.3}$$

with s being the Laplace variable. Before presenting the main convergence theorem, we prove the following auxiliary result .

Lemma 3.1. *We have the identity:*

$$\chi(\alpha,\beta,t) = \begin{cases} \delta(t-\beta) - \frac{\alpha\beta}{\sqrt{t^2-\beta^2}} J_1\left(\alpha\sqrt{t^2-\beta^2}\right), & t\geq\beta,\\ 0, & 0<t<\beta, \end{cases}$$

where δ is the dirac delta function and J_1 is the Bessel function of first order given by

$$J_1(z) = \frac{1}{\pi}\int_0^\pi \cos\left(z\sin\varphi-\varphi\right)d\varphi.$$

Proof. Using the change of variable $r=\sqrt{s^2+\alpha^2}$ we write

$$e^{-\beta r} = e^{-\beta s} - (e^{-\beta s} - e^{-\beta r}).$$

From the table [27, p. 245] we get

$$\mathcal{L}^{-1}\left\{e^{-\beta s}\right\} = \delta(t-\beta), \tag{3.4}$$

Also on page 263 of [27] we find

$$\mathcal{L}^{-1}\left\{e^{-\beta s}-e^{-\beta r}\right\} = \begin{cases} \frac{\alpha\beta}{\sqrt{t^2-\beta^2}} J_1\left(\alpha\sqrt{t^2-\beta^2}\right), & t>\beta,\\ 0, & 0<t<\beta. \end{cases} \tag{3.5}$$

Subtracting (3.5) from (3.4) we obtain the expected inverse Laplace transform. ☐

Now we are ready to prove the convergence result for NNWR in 2D:

Theorem 3.2 (Convergence of NNWR in 2D). *Let $\theta = 1/4$. For $T>0$ fixed, the NNWR algorithm (3.1) converges in $k+1$ iterations, if the time window length T satisfies $T/k < 2h_{\min}/c$, c being the wave speed.*

Proof. We take Laplace transforms in t of (3.2) to get

$$(s^2+c^2n^2)\hat{U}_i^k - c^2\frac{d^2\hat{U}_i^k}{dx^2} = 0,$$

and now treat each n as in the one-dimensional analysis in the proof of Theorem 2.1, where the recurrence relations (2.9), (2.10) and (2.11) of the form

$$\hat{w}_i^k(s) = \sum_j A_{ij}^{(k)}(s)\hat{w}_j^0(s) \tag{3.6}$$

now become for each $n=1,2,\ldots$

$$\hat{W}_i^k(n,s) = \sum_j A_{ij}^{(k)}\left(\sqrt{s^2+c^2n^2}\right)\hat{W}_j^0(n,s). \tag{3.7}$$

The equation (3.6) is of the form (2.14)-(2.15), that means $A_{ij}^{(k)}(s)$ are linear combination of terms of the form $e^{-\varrho s}$ for $\varrho \geq 2kh_l/c$ for some $l \in \{1,2,\dots N\}$. Therefore the coefficients $A_{ij}^{(k)}\left(\sqrt{s^2+c^2n^2}\right)$ are sum of exponential functions of the form $e^{-\varrho\sqrt{s^2+c^2n^2}}$ for $\varrho \geq 2kh_l/c$. Hence we use the definition of χ in (3.3) to take the inverse Laplace transform of (3.7), and obtain

$$W_i^k(n,t) = \sum_j \sum_m \chi(cn, \varrho_{m,j}, t) * W_j^0(n,t),$$

with $\varrho_{m,j} \geq 2kh_{\min}/c$. So it is straightforward that for $t < 2kh_{\min}/c$, $W_i^k(n,t) = 0$ for each n, since the function χ is zero there by Lemma 3.1. Therefore the interface functions $w_i^k(y,t)$, given by $w_i^k(y,t) = \sum_{n\geq 1} W_i^k(n,t)\sin(ny)$ are also zero for all $i \in \{1,\dots,N-1\}$. Hence one more iteration produces the desired solution on the entire domain. ∎

4. Numerical Experiments. We perform numerical experiments to see the convergence behavior of the NNWR algorithm with multiple subdomains for the model problem

$$\begin{aligned} \partial_{tt}u &= c^2(x)\partial_{xx}u, && x \in (0,5), t > 0,\\ u(x,0) &= 0,\ u_t(x,0) = 0, && 0 < x < 5, \\ u(0,t) &= t^2,\ u(5,t) = t^2 e^{-t}, && t > 0, \end{aligned} \tag{4.1}$$

which is discretized using centered finite differences in both space and time on a grid with $\Delta x = \Delta t = 2{\times}10^{-2}$. We consider a decomposition of $(0,5)$ into five unequal subdomains, whose widths h_i are $0.6, 0.6, 0.5, 2.3, 1$ respectively, and take the initial guesses $w_j^0(t) = t^2, t \in (0,T]$ for $1 \leq j \leq 4$. Note that in some of the experiments below, the coefficient $c(x)$ will be spatially varying. This will allow us to study how spatially varying coefficients affect the performance of the NNWR, which have only been analyzed in the constant coefficient case. For the first experiment, we take the constant speed, $c = 1$. On the left panel of Figure 4.1, we show the convergence for different values of the parameter θ for $T = 8$, and on the right the results for the best parameter $\theta = 1/4$ for different time window length T. We observe two-step convergence for $\theta = 1/4$ for a sufficiently small time window T. Now we take the propagation speed, $c(x) = (x+1)/6$ for the second experiment. On the left panel of Figure 4.2, we show the convergence for different values of the parameter θ for $T = 8$, and on the right the results for the best parameter $\theta = 1/4$ for different time window length T.

Next we show an experiment for the NNWR algorithm in two dimension for the following model problem

$$\partial_{tt}u - (\partial_{xx}u + \partial_{yy}u) = 0, u(x,y,0) = xy(x-1)(y-\pi)(5x-2)(4x-3), u_t(x,y,0) = 0,$$

with homogeneous Dirichlet boundary conditions. We discretize the wave equation using the centered finite difference in both space and time (Leapfrog scheme) on a grid with $\Delta x = 5{\times}10^{-2}, \Delta y = 16{\times}10^{-2}, \Delta t = 4{\times}10^{-2}$. We decompose our domain $\Omega := (0,1)\times(0,\pi)$ into three non-overlapping subdomains $\Omega_1 = (0,2/5)\times(0,\pi)$, $\Omega_2 = (2/5,3/4)\times(0,\pi)$, $\Omega_3 = (3/4,1)\times(0,\pi)$. As initial guesses, we take $w_i^0(y,t) = t\sin(y)$. In Figure 4.3 we plot the convergence curves for different values of the parameter θ for

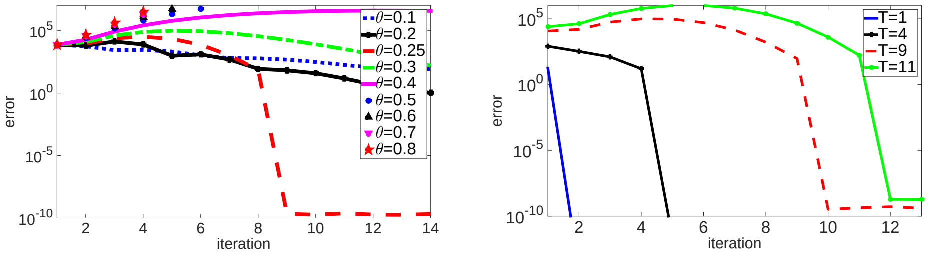

Fig. 4.1: Convergence of NNWR with various values of θ for $T = 8$ on the left, and for various lengths T of the time window and $\theta = 1/4$ on the right

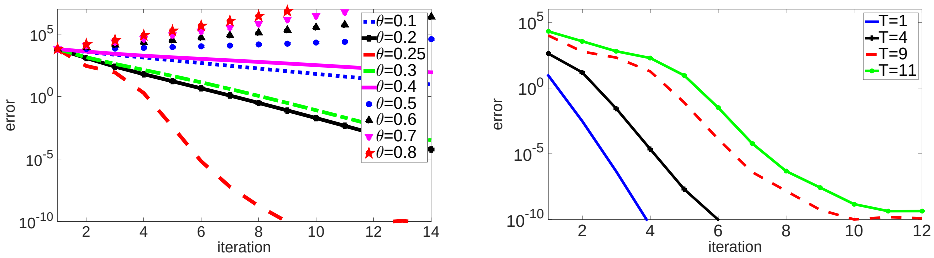

Fig. 4.2: Convergence of NNWR for variable coefficients $c(x) = (x+1)/6$ with various values of θ for $T = 8$ on the left, and for various lengths T of the time window and $\theta = 1/4$ on the right

$T = 2$ on the left panel, and on the right the results for the best parameter $\theta = 1/4$ for different time window length T.

We compare in Figure 4.4 the performance of the NNWR and DNWR (see [12]) algorithms with the SWR algorithms with and without overlap. Here we consider the problem

$$\begin{aligned} \partial_{tt}u - \partial_{xx}u &= 0, && x \in (-3, 2), t > 0, \\ u(x, 0) = 0,\ u_t(x, 0) &= xe^{-x}, && -3 < x < 2, \\ u(-3, t) = -3e^{3}t,\ u(2, t) &= 2te^{-2}, && t > 0, \end{aligned}$$

and for the overlapping Schwarz variant we use an overlap of length $24\Delta x$, where $\Delta x = 1/50$. For the DNWR, NNWR and non-overlapping SWR we consider a domain decomposition into two subdomains $\Omega_1 = (-3, 0)$ and $\Omega_2 = (0, 2)$. We observe that the DNWR and NNWR algorithms converge as fast as the Schwarz WR algorithms for smaller time windows T. Due to the local nature of the Dirichlet-to-Neumann operator in 1D [8], SWR converges in a finite number of iterations just like DNWR and NNWR. In higher dimensions, however, non-overlapping SWR will no longer converge in a finite number of steps, but DNWR and NNWR will; see Figure 4.5. Table 4.1 gives a summary of the theoretical results from Section 2 and 3 and [12], to indicate the maximum number of iterations needed for the 1D and 2D wave equation to converge to the exact solution. For the comparison result in 2D, we consider the

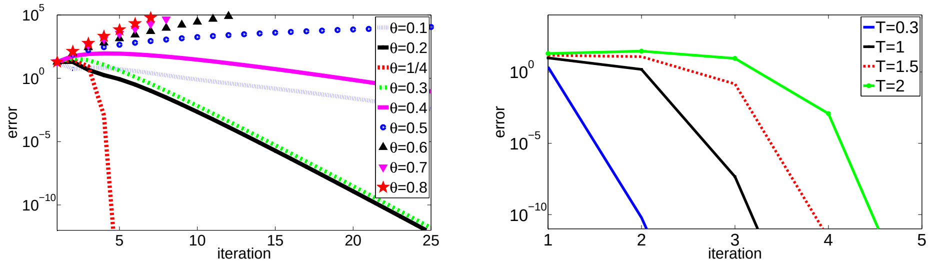

Fig. 4.3: Convergence of NNWR in 2D: curves for different values of θ for $T = 2$ on the left, and for various time lengths T and $\theta = 1/4$ on the right

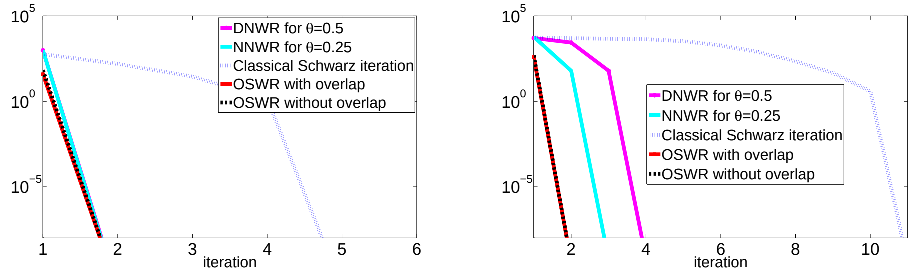

Fig. 4.4: Comparison of DNWR, NNWR, and SWR for 1D wave equation for $T = 4$ on the left, and $T = 10$ on the right

model problem

$$\partial_{tt}u - (\partial_{xx}u + \partial_{yy}u) = 0, u(x, y, 0) = 0 = u_t(x, y, 0),$$

with Dirichlet boundary conditions $u(0, y, t) = t^2 \sin(y), u(1, y, t) = y(y - \pi)t^3$ and $u(x, 0, t) = 0 = u(x, \pi, t)$. We decompose our domain $\Omega := (0, 1) \times (0, \pi)$ for the two subdomains experiment into $\Omega_1 = (0, 3/5) \times (0, \pi)$ and $\Omega_2 = (3/5, 1) \times (0, \pi)$, and for the three subdomains experiment into $\Omega_1 = (0, 2/5) \times (0, \pi)$, $\Omega_2 = (2/5, 3/4) \times (0, \pi)$, $\Omega_3 = (3/4, 1) \times (0, \pi)$. We take a random initial guess to start the iteration, and for the overlapping SWR we use an overlap of length $2\Delta x$ in all the experiments. We implement first order methods with one parameter in optimized SWR iterations; for more details see [5]. On the left panel of Figure 4.5 we plot the comparison curves for two subdomains, and the same for three subdomains on the right.

Now we show a numerical experiment for the NNWR algorithm with different time grids for different subdomains and discontinuous wave speed across interfaces. We consider the model problem

$$\partial_{tt}u - c^2\partial_{xx}u = 0, u(x, 0) = 0 = u_t(x, 0),$$

with Dirichlet boundary conditions $u(0, t) = t^2, u(6, t) = t^3$. Suppose the spatial domain $\Omega := (0, 6)$ is decomposed into three equal subdomains $\Omega_i, i = 1, 2, 3$, and the random initial guesses are used to start the NNWR iteration. For the spatial discretization, we take a uniform mesh with size $\Delta x = 1{\times}10^{-1}$, and for the time discretization, we use non-uniform time grids $\Delta t_i, i = 1, 2, 3$, as given in Table 4.2.

Table 4.1: Comparison of steps needed for convergence for 1D wave equation.

Methods	2 subdomains, 1D	Many subdomains, 1D	Many subdomains, 2D
DNWR	$T \leq 2kh_{\min}/c$	$T \leq kh_{\min}/c$	$T < kh_{\min}/c$
NNWR	$T \leq 4kh_{\min}/c$	$T \leq 2kh_{\min}/c$	$T < 2kh_{\min}/c$

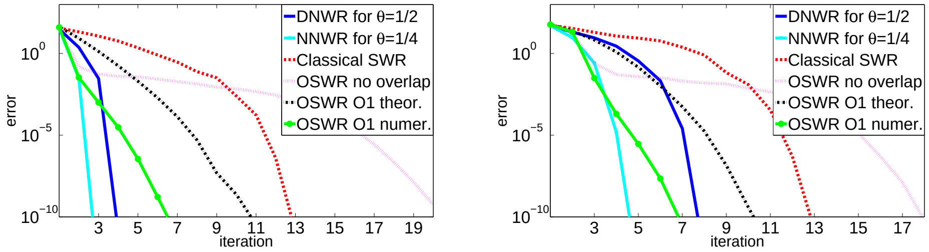

Fig. 4.5: Comparison of DNWR, NNWR, and SWR for $T = 2$ in 2D for two subdomains on the left, and three subdomains on the right

For the non-uniform mesh grid, boundary data is transmitted from one subdomain to a neighboring subdomain by introducing a suitable time projection. For two dimensional problems, the interface is one dimensional. Using ideas of merge sort one can compute the projection with linear cost, see [9] and the references therein. Even for higher dimensional interfaces, such an algorithm with linear complexity is still possible, see [10]. In Figure 4.6 we show the non-uniform time steps for different subdomains. Figure 4.7 gives the convergence behavior of the NNWR algorithm for $T = 2$ with the same non-uniform time grids as in Table 4.2.

Finally we raise the issue of scalability of the NNWR algorithm by giving some numerical examples for the wave equation. From Theorem 2.1, one can say that as long as h/T is constant, we expect identical convergence behavior of the NNWR algorithm. We plot in Figure 4.8 the convergence curves by doubling the number of subdomains and making the time window length half. One can therefore conclude that the NNWR algorithm is weakly scalable for the wave equation.

5. Conclusions . We defined the NNWR algorithm for multiple subdomains and for general hyperbolic problems, and analyzed their convergence properties for the second order wave equation in 1D. We showed using numerical experiments that for a particular choice of the relaxation parameter, more specifically for $\theta = 1/4$, convergence can be achieved in a finite number of steps. In fact, this algorithm can be used as a two-step method, choosing the time window lengh T small enough. We have also extended the NNWR algorithm for the second order wave equation in 2D, and analyzed its convergence properties. We have also shown using numerical experiments that among the DNWR (see [11]) and NNWR methods, NNWR converges faster. But in comparison to DNWR, the NNWR has to solve twice the number of subproblems (once for Dirichlet subproblems, and once for Neumann subproblems) on each subdomain at each iteration. Therefore the computational cost is almost double for the NNWR than for the DNWR algorithm at each step. However, we get better convergence behavior with the NNWR in terms of iteration numbers. Finally we presented a comparison of performences between the DNWR, NNWR and Schwarz

Table 4.2: Propagation speed and time steps for different subdomains.

	Ω_1	Ω_2	Ω_3
wave speed c	$1/4$	2	$1/2$
time grids Δt_i	13×10^{-2}	39×10^{-3}	1×10^{-1}

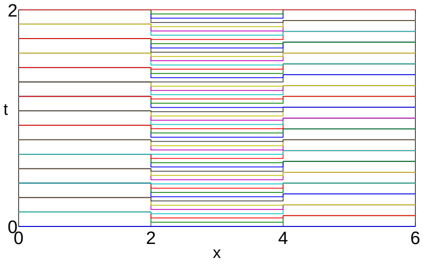

Fig. 4.6: Subdomains with non-uniform time steps

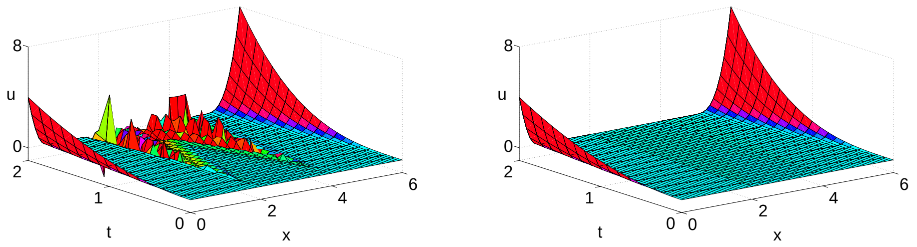

Fig. 4.7: Solution using NNWR method for the wave equation with non-uniform time steps for $\theta = 1/4$ for $T = 2$: Solution after 1st iteration on the left, and solution after 2nd iteration on the right

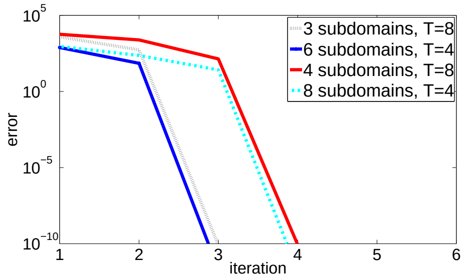

Fig. 4.8: Graphs for comparing scalability of NNWR method for the wave equation

WR methods, and showed that the DNWR and NNWR converge faster than optimized SWR at least for higher dimensions.

Acknowledgement. I would like to express my gratitude to Prof. Martin J. Gander and Prof. Felix Kwok for their constant support and stimulating suggestions.

REFERENCES

[1] J. F. Bourgat, R. Glowinski, P. L. Tallec, and M. Vidrascu, *Variational Formulation and Algorithm for Trace Operator in Domain Decomposition Calculations*, in Domain Decomposition Methods, T. F. Chan, R. Glowinski, J. Périaux, and O. B. Widlund, eds., SIAM, 1989, pp. 3–16.

[2] X.-C. Cai, *Additive Schwarz algorithms for parabolic convection-diffusion equations*, Numer. Math., 60 (1991), pp. 41–61.

[3] ———, *Multiplicative Schwarz Methods for Parabolic Problems*, SIAM J. Sci. Comput., 15 (1994), pp. 587–603.

[4] M. J. Gander, *Optimized Schwarz methods*, SIAM J. Numer. Anal., 44 (2006), pp. 699–732.

[5] M. J. Gander and L. Halpern, *Absorbing Boundary Conditions for the Wave Equation and Parallel Computing*, Math. of Comput., 74 (2004), pp. 153–176.

[6] ———, *Optimized Schwarz Waveform Relaxation for Advection Reaction Diffusion Problems*, SIAM J. Num. Anal., 45 (2007), pp. 666–697.

[7] M. J. Gander, L. Halpern, and F. Nataf, *Optimal convergence for overlapping and non-overlapping Schwarz waveform relaxation*, in 11th International Conference on Domain Decomposition in Science and Engineering, C.-H. Lai, P. E. Bjørstad, M. Cross, and O. B. Widlund, eds., 1999, pp. 253–260.

[8] ———, *Optimal Schwarz Waveform Relaxation for the One Dimensional Wave Equation*, SIAM J. Num. Anal., 41 (2003), pp. 1643–1681.

[9] M. J. Gander and C. Japhet, *An Algorithm for Non-Matching Grid Projections with Linear Complexity*, in Domain Decomposition in Science and Engineering XVIII, M. Bercovier, M. J. Gander, D. Keyes, and O. Widlund, eds., 2008.

[10] ———, *Algorithm 932: PANG: Software for Non-Matching Grid Projections in 2d and 3d with Linear Complexity*, ACM Transactions on Mathematical Software (TOMS), 40 (2013), pp. 6:1–6:25.

[11] M. J. Gander, F. Kwok, and B. C. Mandal, *Dirichlet-Neumann Waveform Relaxation Method for the 1D and 2D Heat and Wave Equations in Multiple subdomains*, in Preparation.

[12] ———, *Dirichlet-Neumann and Neumann-Neumann Waveform Relaxation for the Wave Equation*, in Domain Decomposition in Science and Engineering XXII, Springer-Verlag, 2015.

[13] ———, *Dirichlet-Neumann and Neumann-Neumann Waveform Relaxation Algorithms for Parabolic Problems*, submitted, (arXiv:1311.2709).

[14] M. J. Gander and A. M. Stuart, *Space-time continuous analysis of waveform relaxation for the heat equation*, SIAM J. for Sci. Comput., 19 (1998), pp. 2014–2031.

[15] E. Giladi and H. Keller, *Space time domain decomposition for parabolic problems*, Tech. Report 97-4, Center for research on parallel computation CRPC, Caltech, 1997.

[16] J. Janssen and S.: Vandewalle, *Multigrid Waveform Relaxation on Spatial Finite Element Meshes: The Continuous-time Case*, SIAM J. Numer. Anal., 33 (1996), pp. 456–474.

[17] R. Jeltsch and B. Pohl, *Waveform relaxation with overlapping splittings*, SIAM J. Sci. Comput., (1995).

[18] F. Kwok, *Neumann-Neumann Waveform Relaxation for the Time-Dependent Heat Equation*, in Domain Decomposition in Science and Engineering XXI, J. Erhel, M. J. Gander, L. Halpern, G. Pichot, T. Sassi, and O. B. Widlund, eds., vol. 98, Springer-Verlag, 2014, pp. 189–198.

[19] E. Lelarasmee, A. Ruehli, and A. Sangiovanni-Vincentelli, *The waveform relaxation method for time-domain analysis of large scale integrated circuits*, IEEE Trans. Compt.-Aided Design Integr. Circuits Syst., 1 (1982), pp. 131–145.

[20] E. Lindelöf, *Sur l'application des méthodes d'approximations successives à l'étude des intégrales réelles des équations différentielles ordinaires*, Journal de Mathématiques Pures et Appliquées, (1894).

[21] C. Lubich and A. Ostermann, *Multigrid dynamic iteration for parabolic equations*, BIT, 27 (1987), pp. 216–234.

[22] B. C. Mandal, *Convergence Analysis of Substructuring Waveform Relaxation Methods for*

Space-time Problems and Their Application to Optimal Control Problems, 2014. Thesis (Ph.D.)–University of Geneva.

[23] ———, *A Time-Dependent Dirichlet-Neumann Method for the Heat Equation*, in Domain Decomposition in Science and Engineering XXI, J. Erhel, M. J. Gander, L. Halpern, G. Pichot, T. Sassi, and O. B. Widlund, eds., vol. 98, Springer-Verlag, 2014, pp. 467–475.

[24] V. Martin, *An optimized Schwarz waveform relaxation method for unsteady convection diffusion equation*, Appl. Numer. Math., 52 (2005), pp. 401–428.

[25] E. Picard, *Sur l'application des méthodes d'approximations successives à l'étude de certaines équations différentielles ordinaires*, Journal de Mathématiques Pures et Appliquées, (1893).

[26] Y. D. Roeck and P. L. Tallec, *Analysis and Test of a local domain decomposition preconditioner*, in Domain Decomposition Methods for PDEs, I, R. Glowinski et al., ed., Philadelphia, 1991, SIAM, pp. 112–128.

[27] J. L. Schiff, *The Laplace Transform*, Springer, 1991.

[28] P. L. Tallec, Y. D. Roeck, and M. Vidrascu, *Domain decomposition methods for large linearly elliptic three-dimensional problems*, J. of Comput. and App. Math., (1991).

[29] A. Toselli and O. B. Widlund, *Domain Decomposition Methods, Algorithms and Theory*, Springer, 2005.